Carbohydrate Polymers 97 (2013) 650–658

Contents lists available at SciVerse ScienceDirect

Carbohydrate Polymers

journal homepage: www.elsevier.com/locate/carbpol

# Insights into the nanostructure of low-methoxyl pectin–calcium gels

Irit Ventura [a], Joanna Jammal [b], Havazelet Bianco-Peled [a,*]

[a] Department of Chemical Engineering, Technion-Israel Institute of Technology, Haifa 32000, Israel
[b] Department of Biotechnology and Food Engineering, Technion-Israel Institute of Technology, Haifa 32000, Israel

ARTICLE INFO

*Article history:*
Received 22 February 2013
Received in revised form 23 April 2013
Accepted 20 May 2013
Available online 28 May 2013

*Keywords:*
Pectin
Calcium–pectin gels
SAXS
Nanostructure
Swelling
Egg-box model

ABSTRACT

The nanostructure of calcium-low-methoxyl-pectin gels is still not fully understood despite its wide use in food and biomedical devices. In this study we present a comprehensive small angle X-ray scattering (SAXS) analysis of calcium–pectin gels with various calcium concentrations. Several modeling approaches were examined taking into account the contribution from both junction zones and chains between cross-links. The SAXS studies are supplemented by determination of the gels' mechanical properties and swelling behavior. The model of semiflexible chains without excluded volume effects was found to be most suitable for describing calcium–pectin gels. The SAXS analysis suggests that both rod-like junction zones and point-like cross-links between neighboring chains are formed in calcium–pectin gels. Moreover, as the calcium content increases, the number of the rod-like junction zones decreases while the number of the point-like cross-links increases.



## 1. Introduction

Pectin is a complex group of heteropolysaccharides found mainly in primary cell walls and middle lamella of most plants. The exact composition and molecular architecture of pectin is still being debated, although this molecule was discovered over two hundred years ago (Coenen, Bakx, Verhoef, Schols, & Voragen, 2007; Vincken et al., 2003). At present, the most accepted structure describes a linear backbone composed of (1 → 4)-linked-α-D-galacturonic acid (GalA) units, some of which are naturally methylesterified at position 6 or acetylated at position 2 and/or 3. These homogalacturonans are interrupted by branched residues carrying natural sugars side chains, predominantly galactose, arabinose and xylose (Alistair, Stephen, & Williams, 2006). The percentage of GalA residues that are methylesterified is defined as the degree of methylesterification (DM) and is considered to be a key parameter determining pectin functionality. Pectins in which the DM is higher than 50% are usually classified as high methylester content (HM) pectins and pectins in which the DM < 50% are usually classified as low methylester content (LM) pectins (Sriamornsak, 2003). Commercially, pectin is mostly produced from citrus peel or apple pomace, both by-products of juice production (Rolin, 2002). Pectin is widely used in the food industry as a texturizer or stabilizer. In addition, applications in the area of pharmaceutical and biomedical engineering have recently emerged (Liu, Fishman, & Hicks, 2007; Munarin, Tanzi, & Petrini, 2012).

Many functional attributes of pectin are based on its ability to form gels. The conditions required for gelation depend on the percentage of the methylester groups in the pectin. HM pectin can only form gels in the presence of sugars and an acidic environment, whereas the presence of divalent ions such as calcium induces LM pectin to form gels (Thibault & Ralet, 2003). Traditionally, the formation of $Ca^{2+}$–pectin gels has been described by the "egg-box" mode (Morris, Powell, Gidley, & Rees, 1982; Powell, Morris, Gidley, & Rees, 1982) originally suggested for alginates (Grant, Morris, Rees, Smith, & Thom, 1973). According to this model, cross-links are formed by calcium ions occupying electronegative cavities in the twofold buckled ribbon structure of the non methylesterfied residues. The mechanism of binding involves two or more chains; it is cooperative and leads to the formation of junction zones rather than point-like cross-links. In order to form a stable junction zone, there is a requirement of a minimal length of subsequent non methylesterfied units, estimated to be between 6 (Luzio & Cameron, 2008) and 20 (Braccini & Perez, 2001). The "egg box" model postulated a two-stage process consisting of an initial dimerization and subsequent aggregation of these pre-formed dimes (Powell et al., 1982). A modified model for pectin–calcium gels, termed the "shifted egg-box" model (Braccini & Perez, 2001), was suggested based on a molecular modeling simulation study. This model was purported to provide a better description of these systems since in pectin–calcium gels, a small change in the dimmer conformation (as opposed to alginate) occurs where one chain is slightly shifted with respect to the other. Recent studies have shown that in

* Corresponding author. Tel.: +972 4 8293588; fax: +972 4 8295672.
*E-mail address:* bianco@tx.technion.ac.il (H. Bianco-Peled).

0144-8617/$ – see front matter © 2013 Elsevier Ltd. All rights reserved.
http://dx.doi.org/10.1016/j.carbpol.2013.05.055

**Table 1**
Pectins used in this study.

| $M_w$[b] (kDa) | Origin | GalA[a] (%) | DE[a] (%) | Sample name | Commercial name |
|---|---|---|---|---|---|
| 89 | Citrus | 86 | 34 | CU34 | Classic CU-L 052/11 |
| 67 | Apple | 83 | 34 | AU34 | Classic AU 710 |
| 80 | Apple | 84 | 41 | AU41 | Classic AU 701 |
| 83 | Apple | 86 | 45 | AU45 | Classic AU-L 050/11 |

some cases, in addition to or instead of dimerization, $Ca^{2+}$ ions can interact with single dissociated carboxyl groups, forming mono-complexes by charge reversal on a single chain thus creating an unspecific or random cross-linking between the pectin chains (Fang et al., 2008; Kastner, Einhorn-Stoll, & Senge, 2012; Siew, Williams, & Young, 2005).

The main objective of the current research is to apply small angle X-ray scattering (SAXS) in order to better understand the gel structure of $Ca^{2+}$–LM pectin gels. SAXS is an accurate and non-destructive analytical method for the characterization of structural features in the size range of 1–100 nm (Glatter & Kratky, 1982). Several research papers describe SAXS investigations supporting the "egg-box" structure of alginate gels (Draget et al., 2001; Li, Fang, Vreeker, Appelqvist & Mendes, 2007; Stokke et al., 2000); however, similar studies related to pectin are scarce. Early SAXS studies applied a Kratky analysis to data from gels and identified rod-like objects, postulated to be junction zones (Axelos, 1990; Axelos, Garnier, Renard, & Thibault, 1996). The cross-section of these objects increased with calcium concentration, up to a maximum value of 18 Å. A recent SAXS study of calcium–pectin gels applied a Guinier analysis and estimated cross-sectional radius of gyration values smaller than 8.5 Å. Molecular modeling allowed estimation of the number of chains involved in junction zone formation (Schuster, Cucheval, Lundin, & Williams, 2011). A small angle neutron scattering (SANS) study, which investigated the local conformation of LM pectins in solutions and gels using SANS (Durand et al., 1990), applied the Kratky method and estimated the persistence length (lp) of the polymer at between 60 and 90 Å.

For our SAXS study of $Ca^{2+}$–LM pectin gels, we used several modeling approaches taking into account the contribution from both the junction zones and chains between cross-links. The SAXS studies are supplemented by determination of mechanical properties and swelling properties of the gels, seeking possible relationships between the structure on a local scale and macroscopic properties. Revealing and understanding the gel nanostructure and its influence on the gel properties is a necessary step toward developing existing and opening new engineering opportunities associated with these important materials.

## 2. Materials and methods

### 2.1. Materials

Pectins (for details, see Table 1) were kindly provided by Herbstreith & Fox KG (Germany). $CaCl_2$ was purchased from J.T. Baker. D(+)-Gluconic acid D-lactone (GDL) and ethylene glycol tetraacetic acid (EGTA) was purchased from Fluka. Milli-Q water was used for gel preparation and swelling measurements. All chemical were used as received.

### 2.2. Molecular weight determination

The molecular weight of pectins was evaluated by intrinsic viscosity analysis according to previously published procedures (Hourdet & Muller, 1991). Briefly, pectin samples were dissolved in 0.1 M NaCl at 25 °C and pH 7. The average viscosimetric molecular weight was calculated by applying the Mark–Houwink equation where $K = 0.0436$, $\alpha = 0.78$ (Garnier, Axelos, & Thibault, 1993).

### 2.3. Preparation of $Ca^{2+}$–pectin gels

Cross-linking was performed using a gelation approach that was shown to yield homogenous gels from alginate solutions (Stokke et al., 2000). All $Ca^{2+}$–pectin gels were prepared at the same pectin concentration of 10 mg/ml and at different calcium concentrations represented by the stoichiometry ratio $R$ defined using the ratio between the concentrations of calcium ion and the non-methoxylated GalA residues as $R = 2[Ca^{2+}]/[COO^-]$ (Fraeye, Duvetter, Doungla, Van Loey, & Hendrickx, 2010; Garnier, Axelos, & Thibault, 1993; Strom et al., 2007). Pectin stock solutions at a concentration of 20 mg/ml were prepared by dissolving the appropriate amount of pectin in hot water (60–70 °C) and stirring overnight. $Ca^{2+}$–pectin gels were prepared by adjusting the pH of stock solution to 6 by the addition of NaOH followed by immediately diluting with freshly prepared GDL solution. The concentration of the GDL was calculated to give a stoichiometric ratio of $[GDL] = 2[Ca^{2+}]$. Finally, an appropriate amount of calcium was added from a 100 mM Ca-EDGT stock solution, which was prepared as describe elsewhere (Stokke et al., 2000). The final solution was mixed for a few seconds and then loaded into molds and left overnight to complete gelation.

### 2.4. SAXS

Samples for SAXS measurements were prepared by pouring a solution containing pectin, GDL and Ca-EDGT (see Section 2.3) into a thin-walled glass capillary glass having 0.01 mm wall thickness and 2 mm diameter. The solution was cured overnight to complete gelation. SAXS measurements were performed using a small-angle Molecular Metrology SAXS diffractometer system with Cu Kα radiation from a sealed microfocus tube (MicroMax-002+S), two Göbel mirrors, and three-pinhole slits. The generator powered at 45 kV and 0.9 mA. SAXS patterns were collected using a two-dimensional position sensitive wire detector (20 cm × 20 cm gas-filled proportional type of Gabriel design with resolution of 200 μm), which was located at a distance of 150 cm from the sample. The scattered intensity $I(q)$ was recorded in the range of $0.008 < q < 0.25$ Å$^{-1}$, where $q$ is the scattering vector defined as $q = (4\pi/\lambda)\sin(\theta)$, where $2\theta$ is the scattering angle and $\lambda$ is the radiation wavelength (1.542 Å). The sample capillary was placed in the instrument cell and the measurements were performed under vacuum at $T = 293$ K. Data analysis was performed using home-made software written in Matlab (Josef & Bianco-Peled, 2012). The scattering curves were normalized by subtracting the solvent scattering, as well as correcting for counting time and sample absorption.

### 2.5. Mechanical properties

Samples for mechanical characterizations were prepared by transferring 600 μl of solution containing pectin, GDL and Ca-EDGT (see Section 2.3) into a 14 mm diameter Teflon ring mold and left covered overnight to complete gelation. The mechanical

properties of the gels were measured using a Lloyd tensile machine in compression mode. The samples were compressed at a constant deformation rate of 25 mm/min. The Young's modulus, $E$, was determined from the slope at the linear region of the stress–strain curve, typically between 1% and 10% extensions (Krupa, Nedelcev, Racko, & Lacik, 2010). The final average values and standard deviations were obtained from the analysis of at least eight measurements. Characterization of swollen gels was performed using the same procedure; however, the samples were immersed in water until reaching equilibrium (see Section 2.6). The shear modulus $G$ was assumed to be given by $G \approx E/3$ (Rubinstein & Colby, 2003). Statistical tests (one-way ANOVA) were applied to Young's modulus values and to data from swelling tests. In all the analyses, the level of significance was set at $p < 0.05$.

### 2.6. Swelling experiment

Samples were prepared as described in Section 2.5. In order to determine the time required for swelling equilibrium, Kinetics experiments were performed first. These were followed by experiments aimed at determining the swelling degree at equilibrium (Davidovich-Pinhas & Bianco-Peled, 2010). $Ca^{2+}$–pectin gel tablets were placed on a stainless steel grid submerged in a Petri dish containing 50 ml water that was covered during the experiment in order to minimize water loss caused by evaporation. At least eight tablets were tested for each calcium concentration. The kinetics of the hydrogel swelling was tested by periodically measuring the weight of each tablet separately and immediately returning the gels to the plate until the next weighing. Pectin samples were found to reach equilibrium after a swelling time of no more than 1440 min. The equilibrium swelling tests used the same method described above but here the samples were weighed only at the beginning of the experiment and after sufficient time had passed so that equilibrium determined from the kinetics tests was achieved. The final values and standard deviations were averaged for each calcium concentration.

## 3. Results and discussion

### 3.1. Nanostructure investigation

Calcium–pectin hydrogels with no added salt, constant pectin concentration of 10 mg/ml and different calcium/pectin ratios were studied by SAXS. The study design included investigation of three apple pectin samples with varying DM (DM = 34, 41 and 45) in order to assess the influence of DM on the nanostructure. In addition, we included an additional sample from citrus with DM of 34, in order to examine the influence of the pectin origin.

#### 3.1.1. Selecting a model for data analysis

Since, traditionally, LM pectin is believed to be structurally similar to alginate gels (Morris et al., 1982; Powell et al., 1982), we initially attempted to fit the experimental data using the broken rod model (Stokke et al., 2000), which was successfully applied for calcium-alginate gels (Stokke et al., 2000). This model allows polydispersity of the junction zone dimensions by taking into account contributions from two long rod-like components representing the junction zones, each having a cross-section radius of $R_i$, and a relative weight of $k_i$.

$$I(q) = \sum_{i=1}^{2} \left[ k_i \cdot q^{-1} \frac{{J_1}^2(qR_i)}{(qR_i)^2} \right] + k_3 q^{-2} \quad (1)$$

where $J_1$ is the first order Bessel function and $k_3$ represents the random spatial correlation between components.

The broken rod model provided a good fit to scattering profiles of Ca–pectin gels (as demonstrated in Fig. S1 in the supplementary information for a representative sample). For most samples tested, radii of around 5 Å and 20 Å were obtained. In line with previous studies of Ca-alignate gels, these values could be attributed to the radii of a dimmer and an assembly of junction zones formed from several chains, respectively (Stokke et al., 2000). A critical examination of the fitted parameters, nevertheless, raised some concerns. First, in about 20% of the samples, fitted values lower than 4 Å were obtained—which are smaller than the diameter of a single sugar ring (about 4.35 Å (Durand et al., 1990). Another limitation of this model was its high sensitivity to the values used as an initial guess. In some cases, the fitted parameter obtained from two runs with different initial guesses differed in almost an order of magnitude (data not shown). Reducing the number of parameters in the "broken rod" by using only one rod ($n = 1$ in Eq. (1)) did not improve model sensitivity, and in many cases radii of 1.5–3 Å was obtained. Therefore, we concluded that the broken rod model is not suitable to describe scattering from pectin gels. It is noted that the shifted egg-box model (Braccini & Perez, 2001), which is supposed to provide a better discription of pectin gels, is identical to the egg-box model on the nanometric scale since they both describe an elongated rod. Consequently, separate calculations was not required for this model.

Supplementary data associated with this article can be found, in the online version, at http://dx.doi.org/10.1016/j.carbpol.2013.05.055.

Another model, commonly used to describe the scattering intensity from polymer gels, takes into account a solution-like contribution, often described by the Orenstein–Zernike equation (Cohen, Ramon, Kopelman, & Mizrahi, 1992), and an excess scattering term representing inhomogeneities in the gels, often described by the Debye–Bueche function (Debye & Bueche, 1949). The combined model is given by

$$I(q) = \frac{K_{net}}{1 + q^2 \xi_{net}^2} + \frac{K_{agg}}{(1 + q^2 \Xi_{agg}^2)^2} \quad (2)$$

where $\xi_{net}$ is the correlation length (or the "mesh size"), $\Xi_{agg}$ is the typical size of inhomogeneities in the gel, and $K_{net}$ and $K_{agg}$ are the corresponding relative weights. The fit of model to the data was not satisfying (Fig. S1 in supplementary information), in particular in the small q range where $q < 0.05$. As a result, we attempted to replace the inhomogeneities term in Eq. (2) with long rod-like components representing the junction, analogous to the broken rod model:

$$I(q) = \frac{K_{net}}{1 + q^2 \xi_{net}^2} + K_1 \cdot q^{-1} \frac{{J_1}^2(qR_1)}{(qR_1)^2} \quad (3)$$

This modified model gave a good fit to the experimental data (Fig. S1). However, as in the case of the broken rod model, the fitted radius was in many cases smaller than 5 Å and the sensitivity to the initial guess was still very high.

Based on the above description, we concluded that no physical insights can be deduced from either the broken rod or the two other models represented by Eqs. (2) and (3). We suspected that the limitations of these models were due to inaccurate description of the solution-like contribution. In order to examine this hypothesis, we replaced this term with a more accurate model that take into account both the rigid and flexible character of the chain. We selected a model that was originally developed by Pedersen and Schurtenberger to describe the scattering from semiflexible chains with excluded volume effects (Pedersen & Schurtenberger, 1996) with the alternations suggested by Chen, Butler, and Magid (2006) and that was recently applied to alginate solutions (Josef & Bianco-Peled, 2012). The second term representing the junction zones was

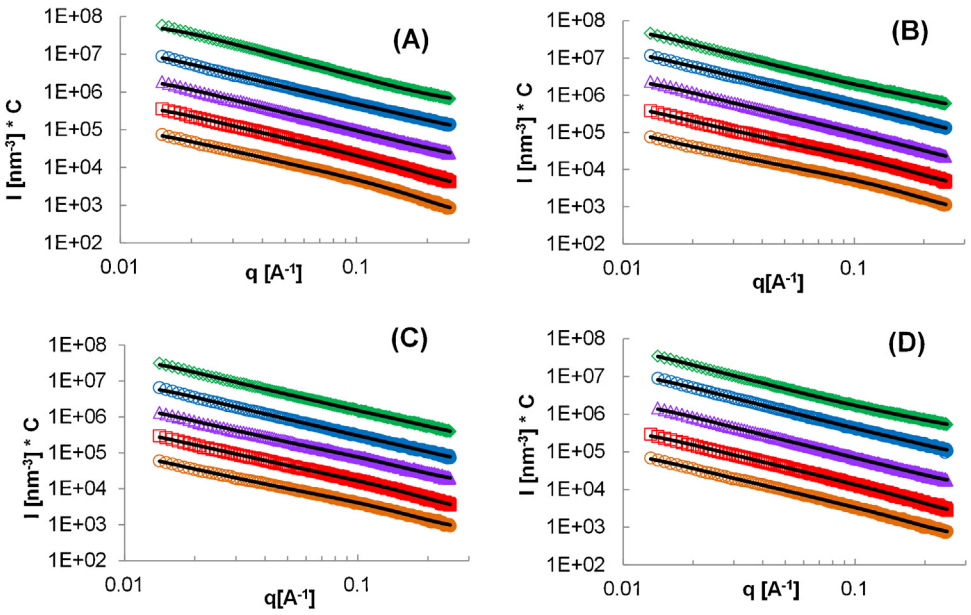


**Fig. 1.** SAXS curves for calcium–pectin hydrogels. (A) AU34, (B) CU34, (C) AU41 and (D) AU45. The calcium concentrations from top to bottom: $R = 3$, 2.5, 2.0, 1.5 and 1.0. The black lines represent fits to Eq. (4). The curves are shifted for better visualization.

adopted from the broken rod model. The equation used to fit the results takes the form:

$$I(q, L, b, r) = K_{\text{chain}} \cdot P(q, b, L) + K_{\text{rod}} \cdot q^{-1} \frac{J_1^2(qr)}{(qr)^2} \tag{4}$$

where $P(q,b,L)$ is given by

$$P(q, b.L) = [1 - w(qR_g)] \cdot P_{\text{Debye}}(q, b, L) + w(qR_g)[C_1(qR_g)^{-1/\nu} \times C_2(qR_g)^{-2/\nu} C_3(qR_g)^{-3/\nu}] + C\left(\frac{L}{b}\right)\frac{b}{15L} \times \left[4 + \frac{7}{u} - \left(11 + \frac{7}{u}\right)e^{-u}\right]$$

where $L$ is the contour length, $b$ is Kuhn's length, $K_{\text{chains}}$ is a constant proportional to the number of polymer chains, $K_{\text{rod}}$ is a constant proportional to the number of the rod-like objects, $r$ is the radius of the rod, and $R_g$ is the radius of gyration of the polymer chain. Details of the functions can be found in Pedersen and Schurtenberger's manuscript (Pedersen & Schurtenberger, 1996). In order to reduce the number of calculated parameters, the contour length was precalculated from the relation

$$L = \frac{M_w \times \%\text{GalA}}{M} l \tag{5}$$

where $M_w$ is the average molecular weight of the pectin, %GalA is the presentge of the linear portion of the chain, $M$ is the molecular weight of the monomeric GalA unit (equal to 194 g/mol) and $l$ is the length of the repeat unit, 4.35 Å (Hourdet & Muller, 1991). Fit of the SAXS data from calcium–pectin hydrogels at different calcium concentrations between $R = 1$–3 in Eq. (4) are presented in Fig. 1. As can be seen, a good fit was obtained for all samples. This model proved to be insensitive to the initial guess of the parameters values.

### 3.1.2. Results of model fitting

Fitting the SAXS profiles to the model of semiflexible chains with rod-like objects enabled us to characterize the two main structural features of pectin gels: Kuhn's length, $b$, characteristic to the polymer's chain flexibility, and the radius of the junction zone $r$. Fig. 2 presents the dependence of these two parameters on the gel's calcium content. The figure also shows the pre-factors $K_{\text{chain}}$ and $K_{\text{rod}}$ representing the relative concentrations of the polymer chains and the junction zones, respectively. For all pectin samples, the Kuhn's length of the hydrogels is larger than the Kuhn's length obtained for pectin solutions, i.e., $R = 0$ (Fig. 2A). These results indicate higher stiffness of polymer chains when found in Ca–pectin gels. The radius of the rod-like objects does not vary considerably with changes in the calcium content or DM (Fig. 2A). The radius was found to be about 12 Å for all samples, the same order of magnitude of dimmer values reported in an early SAXS study (Axelos, 1990) and a more recent molecular simulation (Braccini & Perez, 2001). Traditionally, Ca-induced gelation is considered to be a two-stage process with initial dimerization and subsequent aggregation of these dimmers. However, the constant dimension of the rod-like objects suggests that either no dimmer association occurs or that the process does not depend on the calcium concentration. Previous studies suggested that the first suggestion is more likely to occur in pectins. ITC studies detected three thermal processes occurring when calcium with increasing concentrations was added to the alginate. The first process was described as monocomplexation, the second as dimerization and the third as lateral association, i.e., aggregation of dimmers (Fang et al., 2008, 2007). In contrast, only two thermal transitions, attributed to monocomplexation and dimerization, were observed in pectins (Fang et al., 2008). Molecular modeling study concluded that dimers aggregation may occur in Ca–pectin gels, but the formed aggregates were weaker associations that are less specific, governed by electrostatic interactions (Braccini & Perez, 2001). Schuster et al. studied a series of pectin gels and in some of the cases lateral aggregation of the dimmers were not found (Schuster et al., 2011).

The weighting factors of the polymer chains are larger by two orders of magnitude from those of the rod-like objects (Fig. 2C and D). Therefore, it was of interest to analyze the relative contribution of each term to the total scattering intensity and overrule the possibility that the scattering is dominated by the solution-like contribution. Fig. 3 displays a typical fit of the data to the model along with the contributions of both terms. It can be seen that even though the contribution of scattering from the rod-like junction zones is somewhat larger than the contribution of the polymer chains, it is not negligible.

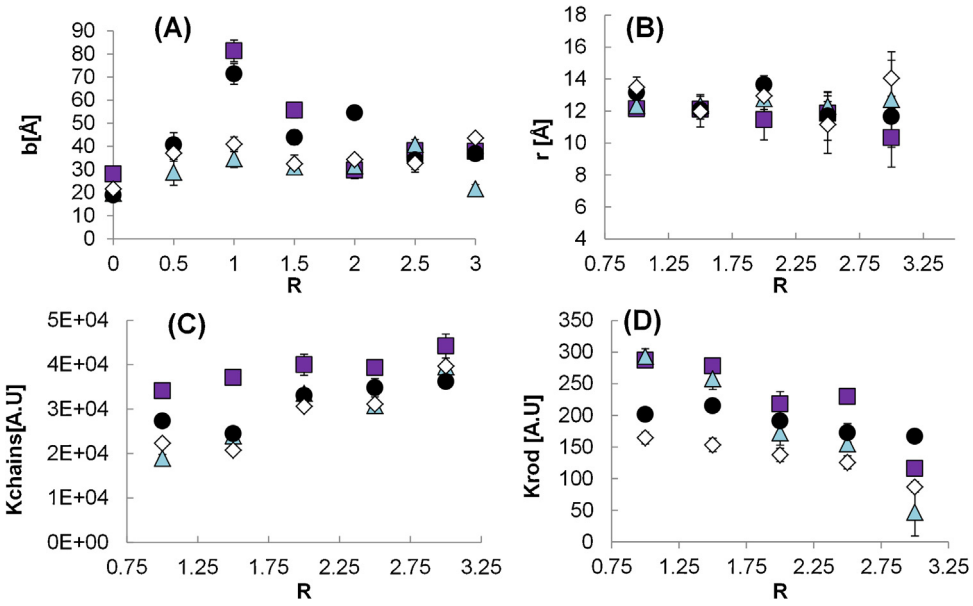


**Fig. 2.** Dependence of (A) Kuh'n length, *b*, (B) The radius of the junction zone *r*, (C) $K_{chains}$, and (D) $K_{rod}$ on the relative calcium concentration *R*. (■) CU34, (▲) AU34, (●) AU41 and (◊) AU45.

Another finding presented in Fig. 2C and D is a pronounced dependence of the weighting factors $K_{rod}$ and $K_{chain}$ on the calcium concentration, observed for all tested pectins. Generally speaking, these pre-factors are proportional to the squared contrast (electron density difference between the scattering object and the medium), the squared volume of the scattering object, and the number of the scattering objects. For $K_{rod}$, the weighting factor of the junction zones, it can be assumed that the electron density difference is constant. Furthermore, since the radius does not depend on the calcium concentration (Fig. 2B), the volume of the scattering object is also constant. Thus, $K_{rod}$ is proportional to the number of the junction zones. It can be seen in Fig. 2C that $K_{rod}$ decreases with calcium concentration for all pectins tested, implying that the larger the calcium concentration, the smaller the number of junction zones. This is a surprising result since the gel strength increases with calcium concentration (Fraeye, Duvetter, et al., 2010), which is presumed to be due to the larger number of cross-links in the formation of junction zones. It is noteworthy that the weighting factor of the term representing the junction zones in alginate gels generally increases with calcium concentration, as expected from a system in which most cross-links are in the form of junction zones (Stokke et al., 2000).

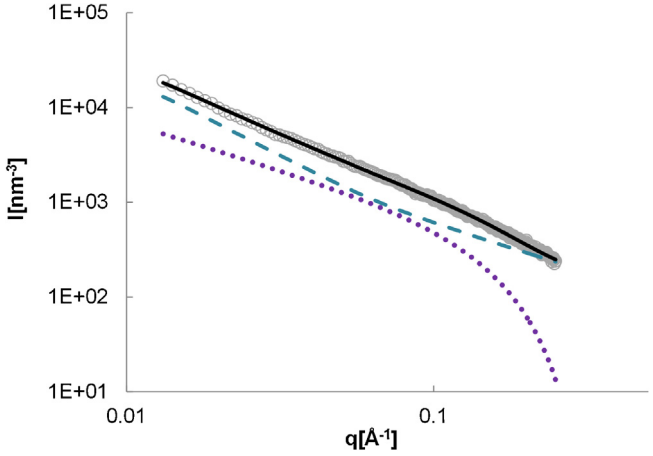


**Fig. 3.** A typical fit of the model to representative SAXS curve, CU34, $R = 1.5$ (open circles). Continuous lines are the fitted model to the scattering curve (continues line) and the two terms constructing it: the rod like junction zones (dashed line) and the polymer chains (dotted line).

Suggesting that an increased calcium concentration reduces the amount of the junction zones unavoidably raises the question of where the excess calcium is located. One possibility is formation of monocomplexes which was previously described by (Fang et al., 2008; Kastner et al., 2012; Siew et al., 2005). Monocomplexes, formed by charge reversal, are composed of few calcium ions and a single pectin chain. The scattering from moncomplexes is expected to be higher than of the bare polysaccharide chains since the electron density of calcium is higher than that of the polymer. The increase in $K_{chain}$ that increases with calcium concentration, observed for all pectin samples (Fig. 2D), indicates that additional monocomplexes are formed as the calcium concentration is increased. Another indication of the formation of monocomplexes is the background scattering that also increases with calcium concentration. Since the polymer concentration was constant in all experiments, increased background scattering implies that contrast is enhanced; see Fig. S2 in the supplementary information. Formation of monocomplexes was previously reported by Siew and Willams, who studied the binding of $Mn^{2+}$ and $Ca^{2+}$ ions to low ester amided pectin, alginate and polyacrylic acid using electron spin resonance spectroscopy (Siew et al., 2005). Alginate and pectin gelation was attributed to formation of polymer–metal complexes involving one or two carboxylate groups resulting in charge reversal or charge annihilation (Siew et al., 2005). Other studies have also suggested that less specific interactions contribute to gel strength (Ngouemazong, Nkemamin, et al., 2012; Ngouamazong et al., 2012; Ngouemazong, Twngweh, et al., 2012).

Supplementary data associated with this article can be found, in the online version, at http://dx.doi.org/10.1016/j.carbpol.2013.05.055.

### 3.1.3. Suggested structural model

The SAXS analysis discussed above suggests that both rod-like junction zones and monocomplexes are indeed formed in calcium–pectin gels. However, monocomplexes, i.e., complexes of

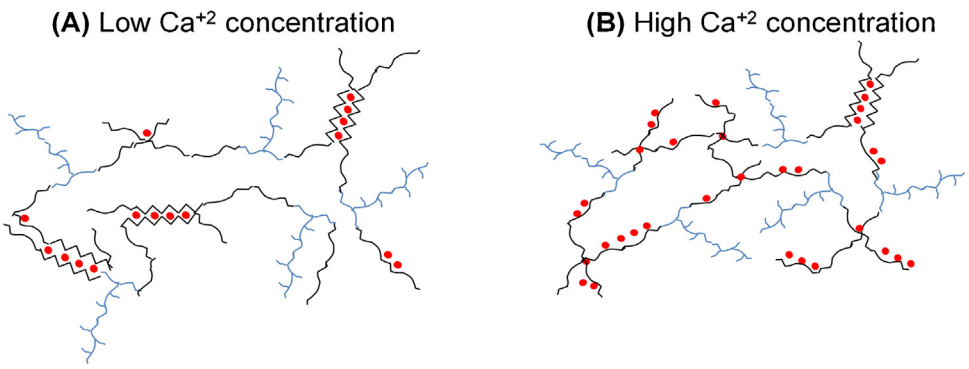


**Fig. 4.** Suggested scheme for calcium–LM pectin gels, based on the nanostructure obtained from the SAXS investigation. (A) Calcium–pectin gel with low calcium concentration. (B) Calcium–pectin gel with high calcium concentration.

a single polymer chain and calcium ions, coexist with the junction zones. Moreover, as the calcium content increases, the number of the junction zones decreases while the number of the monocomplexes increases. It must be emphasized that formation of junction zones involves two or more chains, and therefore, this process contributes to the mechanical stability of the gel. If junction zones are the only route leading to cross-linked networks, one would expect that increasing the calcium content will lead to reduction in gel stiffness due to lower cross-linking densities. Considerable experimental evidence showing an opposite trend (Fraeye, Colle, et al., 2010) implies that cross-linking may take other forms in calcium pectin gels. Cross-linking appears to involve not only junction zone formation but also point-like cross-links between neighboring chains or monocomplexes. These point-like cross-links do not contribute to the scattering intensity due to their small size. The physical picture gathered from the SAXS findings is quite different from the way calcium–pectin hydrogels are commonly described. Furthermore, it is considerably unlike alginate gelation, even though these two types of polysaccharide gels are often described as similar. Fig. 4 presents the suggested scheme for calcium–LM pectin gels, based on nanostructure obtained from comprehensive SAXS investigation. It illustrates the main features of the suggested gelation scheme and its dependence on the calcium concentration. At low calcium concentrations, rod-like junction zones coexist with monocomplexes and point-like cross-linking. At high calcium concentrations, fewer junction zones are found alongside more point-like cross-linking as well as calcium located on the polymer chains. The nanostructure described here, and its differences in gelation in comparison to alginate gelation, is mainly governed by the branched nature of pectins, as opposed to the linear nature of alginate. The pectin backbone contains branched regions (Alistair et al., 2006), which can cause steric constraints and prevent formation of junction zones. In addition, commercial LM pectin, such as the ones used in the current study, are produced industrially from HM pectin by a chemical de-esterification process that results in a random distribution of methyl-ester (Alistair et al., 2006). This random distribution might limit the number of sequences with length exceeding the minimal value required for junction zone formation (Braccini & Perez, 2001; Luzio & Cameron, 2008; Powell et al., 1982). These structural features of pectin and its branched backbone can also explain the lack of the dimmers' lateral associations, which might be prevented due to steric limitations. Thus the molecular level dissimilarity between the branched pectin with randomly distributed residues and the linear alginate characterized by a relatively blockwise distribution of residues is manifested in the gelation mechanism. This conclusion is in line with a previous study that demonstrated some differences in gelation mechanisms of pectin and alginate (Fang et al., 2008).

### 3.2. Physical properties

The physical properties of pectin gels are strongly influenced by several factors. Intrinsic variables of the pectin molecule such as the molecular weight, DM, charge density and the distribution of the methyl ester along the backbone chain are of great importance. Apart from the innate characteristics of pectin, extrinsic factors such as pH, ionic strength, pectin and calcium concentrations and temperature also have an important influence on the strength, texture and viscoelastic properties of $Ca^{2+}$–pectin gels. Although the mechanical properties of $Ca^{2+}$–pectin gels were previously extensively studied (Fraeye, Colle, et al., 2010; Fraeye et al., 2009; Iijima, Hatakeyama, & Hatakeyama, 2005; Strom et al., 2007), investigation relating these parameters to the nanostructure is still missing in the literature.

#### 3.2.1. Young's modulus

The mechanical properties of calcium–pectin hydrogels were characterized in an attempt to correlate them and the gels' nanostructure. Young's modulus is presented in Fig. 5. The stiffest gel was found to be CU34 followed by AU34. Both gels were prepared from pectins with the same DM, 34. The two other samples, with DM of 41 and 45, respectively, had much lower moduli. This result is in line with a previous study reporting that the strength of the LM pectin gels increases when the DM decreases around 25–45% (Kim, Rao, & Smit, 1978). Additionally, for all pectin samples, Young's modulus significantly increased with calcium concentration ($p < 0.05$) up to a relatively constant plateau value. This observation is in agreement with previous works

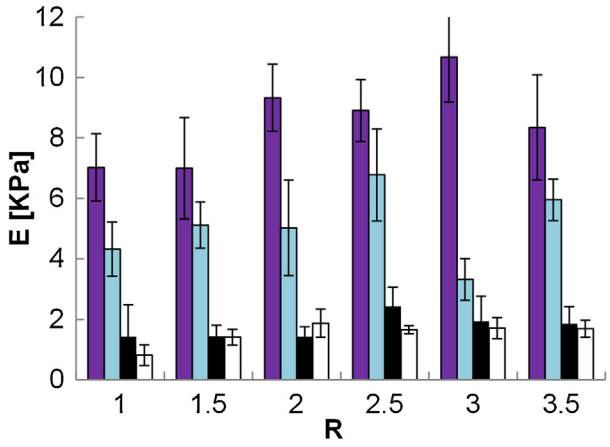


**Fig. 5.** Young's modulus, *E*, as a function of calcium concentration (■) CU34, (■) AU34, (■) AU41 and (□) AU45.

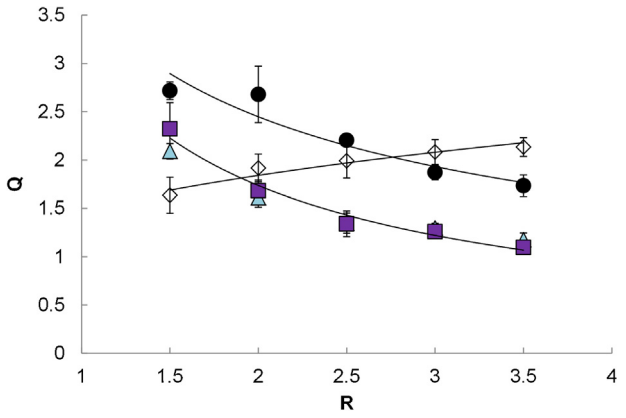


**Fig. 6.** Equilibrium swelling ratios as a function of calcium concentration. (■) CU34, (△) AU34, (●) AU41 and (◊) AU45. The error bars representing the standard deviation are in some cases smaller than the size of the symbols.

showing that above a certain calcium concentration, the gel stiffness will not increase further (Ngouemazong, Nkemamin, et al., 2012; Ngouamazong et al., 2012). The $R$ value at which the maximum was obtained was in the range of $R = 2.5–3$ for all samples.

No clear correlation between Young's modulus and the nanostructural parameters obtained in Section 3.1.2 was found. The hydrogel stiffness depends on many parameters including DM, macromolecular structure of the pectin backbone, the polymer and the calcium concentrations (Alistair et al., 2006). Presumably the influence of these parameters masks the influence of the nanostructure, if such exists.

### 3.2.2. Swelling behavior

Swelling of the hydrogel network is one of its important characteristics. Swelling is driven by the favorable free energy of mixing with a solvent (osmotic pressure) and is resisted by the energy required to stretch network strands (modulus). The swelling reaches an equilibrium state when the osmotic and elastic parts of the free energy balance (Rubinstein & Colby, 2003). It has been previously shown that swelling alginate gels could not be described using classic theories developed for hydrogels with point-like cross-links (Davidovich-Pinhas & Bianco-Peled, 2010). Therefore, the swelling behavior of pectin gels was characterized in an attempt to gain further support for the validity of the nanostructural model describing coexistence of point-like and junction zone cross-links.

The equilibrium swelling ratios as a function of calcium concentration are presented in Fig. 6. We found that the swelling of all studied pectins could be empirically described by a single low exponent power model, $Q = A[R]^n$. The best power values, $n$, of this fit were −0.866, −0.663, −0.583 and 0.377 for CU34, AU34, AU41 and AU45, respectively. This empirical relation has also been fitted previously to alginate swelling, where all alginate tested displayed similar power values of about −0.49 (Davidovich-Pinhas & Bianco-Peled, 2010), which are similar to the values obtained here for all pectins apart from AU45.

Most studied pectins (CU34, AU34 and AU41) display a decrease in the swelling ratio with an increase in calcium concentration. The resemblance in the trend may imply that the swelling mechanism is similar. This behavior is in agreement with a previously reported study by Zsivanovits who examined the swelling behavior of a series of pectin films whose DM and methylester distribution in different salty environments varied (Zsivánovits, Marudova & Ring, 2005). Tibbits, MacDougall, and Ring (1998) also observed increased swelling with decreased calcium concentration in salt solutions. In contrast to the pectins with DM of 34 and 41, the gel with the highest DM (AU45) shows a reverse swelling trend: the swelling ratio increases with the increase in calcium concentration. This unexpected behavior could be attributed to the pectin's high DM. Traditionally, pectins are classified as LM if the DM is lower than 50%. It is possible that a DM of 45% is a borderline value; hence, it is too high to be performing similarly to LM pectin gel. Other experimental studies have also demonstrated critical DM for calcium-mediated gelation occurring at a DM of around 40–45 (Axelos, 1990; Thibault & Rinaudo, 1986). Another point to be mentioned is that the swelling curves obtained for the two pectins with identical DM, AU34 and CU34, were practically identical. This result implies that they share the same swelling mechanism, suggesting that the DM is an important factor determining the swelling behavior. In addition, the swelling of AU41, having a higher DM, is larger than that of AU34 and CU34 with relatively smaller DM, which suggests that the swelling ratio increases with the DM.

Quantification of the swelling results was performed by estimating the number of segments between cross-linking points $N$ based on the relation

$$G = \frac{1}{N}\frac{CRT}{M} \tag{6}$$

where $G$ is the shear modulus, $C$ is the polymer concentration, $R$ is the gas constant and $T$ is the temperature. Eq. (6), was derived from the rubber elasticity theory, originally developed for chemically cross-linked gels (Mitchell, 1980; Rubinstein & Colby, 2003; Treloar, 1975; Van Kleef, Boskamp, & Van Den Tempel, 1978); the specific details can be seen in Rubinstein and Colby (2003).

The shear modulus, $G$, was calculated from Young's modulus $E$ as $G \approx E/3$ (Rubinstein & Colby, 2003). Since Eq. (6) holds only for gels at swelling equilibrium, Young's modulus was measured separately for swollen gels (Fig. 7A).

The number of segments between cross-links is plotted against the equilibrium swelling ratios in Fig. 7B. In the equilibrium swollen state, the gels' modulus increased with calcium concentration while the number of segments between cross-linking decreased

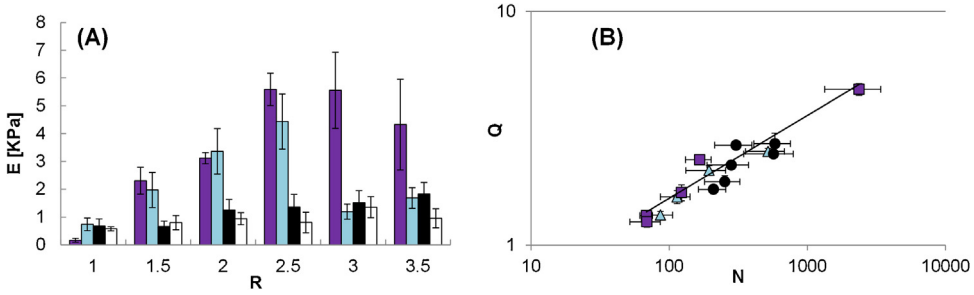


**Fig. 7.** (A) Young's modulus of the gels at their equilibrium-swollen state. (■) CU34, (□) AU34, (■) AU41 and (□)AU45. (B) Equilibrium swelling ratios as a function of cross-linking density on log–log scale. (■) CU34, (△) AU34, (●) AU41 and (◊) AU45. The error bars representing the standard deviation are in some cases smaller than the size of the symbols.

(data is not shown). This result is in agreement with the findings obtained from the SAXS analysis presented in Section 3.2.1.

Another observation made based on Fig. 7B is that the cross-linking density is in direct relation with the swelling ratio, which is in agreement with Flory's classic theory. The data from all pectin gels collapsed into a single line represented by an empirical low power correlation $Q = 0.31N^{0.34}$. On the one hand, this result does not meet the classic swelling theory predicting $Q \approx N^{0.57}$ (Rubinstein & Colby, 2003). On the other hand, the deviation from the classical theory is less extreme compared to alginate gels for which $Q$ decreased with $N$ (Davidovich-Pinhas & Bianco-Peled, 2010). Possibly, the complexity of pectin networks limits their compatibility to the classic theories of Flory and rubber elasticity.

## 4. Conclusions

An extensive SAXS analysis of $Ca^{2+}$–LM pectin gels was performed on three different apple pectins having different DM and one citrus pectin. Several models were examined, all taking into account the contribution from both the junction zones and chains between cross-links. Although the fit quality was good for most models, high sensitivity to the initial guess and interpretation of the physical meaning of fitted parameters were used to eliminate several models. The model of semiflexible chains without excluded volume effects was found to be the most suitable for describing $Ca^{2+}$–LM pectin gels. The SAXS analysis suggests that cross-linking occurs not only through formation of rod-like junction zones but also by point-like cross-links between neighboring chains and monocomplexes. Moreover, as the calcium content increases, the number of the rod-like junction zones decreases while the number of the monocomplexes increases. To the best of our knowledge, this is the first time it has been shown using a structural characterization method that enhancing the calcium concentration does not produce more rod-like junction zones. The SAXS findings indicate a cross-linking mechanism that is quite different from the common description of $Ca^{2+}$–LM pectin gels. Apparently, the cross-linking scheme is mainly governed by the branched nature of pectins, as opposed to the linear nature of alginate. The SAXS studies was supplemented by determination of mechanical properties and swelling behaviors of the gels, which were analyzed using known swelling theories originally developed for chemically cross-linking polymers.

## Acknowledgment

The authors would like to thank Dr. Elinor Josef for fruitful discussions.

## References


Alistair, M., Stephen, G. O. P., & Williams, P. A. (2006). *Food polysaccharides and their applications*. Boca Raton, FL: CRC Press.

Axelos, M. A. V. (1990). Ion complexation of biopolymers: Macromolecular structure and viscoelastic properties of gels. *Makromolekulare Chemie. Macromolecular Symposia*, *39*, 323–328.

Axelos, M. A. V., Garnier, C., Renard, C. M. G. C., & Thibault, J.-F. (1996). Interactions of pectins with multivalent cations: Phase diagrams and structural aspects. In J. Visser, & A. G. J. Voragen (Eds.), *Pectins and pectinases* (pp. 35–45). Amsterdam, the Netherlands: Elsevier.

Braccini, I., & Perez, S. (2001). Molecular basis of $Ca^{2+}$-induced gelation in alginates and pectins: The egg-box model revisited. *Biomacromolecules*, *2*(4), 1089–1096.

Chen, W.-R., Butler, P. D., & Magid, L. J. (2006). Incorporating intermicellar interactions in the fitting of SANS data from cationic wormlike micelles. *Langmuir*, *22*(15), 6539–6548.

Coenen, G., Bakx, E., Verhoef, R., Schols, H., & Voragen, A. (2007). Identification of the connecting linkage between homo- or xylogalacturonan and rhamnogalacturonan type I. *Carbohydrate Polymers*, *70*(2), 224–235.

Cohen, Y., Ramon, O., Kopelman, I. J., & Mizrahi, S. (1992). Characterization of inhomogeneous polyacrylamide hydrogels. *Journal of Polymer Science Part B: Polymer Physics*, *30*(9), 1055–1067.

Davidovich-Pinhas, M., & Bianco-Peled, H. (2010). A quantitative analysis of alginate swelling. *Carbohydrate Polymers*, *79*(4), 1020–1027.

Debye, P., & Bueche, A. M. (1949). Scattering by an inhomogeneous solid. *Journal of Applied Physics*, *20*(6), 518–525.

Draget, K. I., Gassered, O., Aune, I., Andersen, P. O., Storbakken, B., Stokke, B. R. T., et al. (2001). Effects of molecular weight and elastic segment flexibility on syneresis in Ca-alginate gels. *Food Hydrocolloids*, *15*(4–6), 485–490.

Durand, D., Bertrand, C., Busnel, J. P., Emery, J. R., Axelos, M. A. V., Thibault, J., et al. (1990). Physical gelation induced by ionic complexation: Pectin–calcium systems. In W. Burchard, & S. B. Ross-Murphy (Eds.), *Physical networks: Polymers and gels* (pp. 283–300). London: Springer.

Fang, Y., Al-Assaf, S., Phillips, G. O., Nishinari, K., Funami, T., & Williams, P. A. (2008). Binding behavior of calcium to polyuronates: Comparison of pectin with alginate. *Carbohydrate Polymers*, *72*(2), 334–341.

Fang, Y., Al-Assaf, S., Phillips, G. O., Nishinari, K., Funami, T., Williams, P. A., et al. (2007). Multiple steps and critical behaviors of the binding of calcium to alginate. *Journal of Physical Chemistry B*, *111*(10), 2456–2462.

Fraeye, I., Colle, I., Vandevenne, E., Duvetter, T., Van Buggenhout, S., Moldenaers, P., et al. (2010). Influence of pectin structure on texture of pectin–calcium gels. *Innovative Food Science & Emerging Technologies*, *11*(2), 401–409.

Fraeye, I., Doungla, E., Duvetter, T., Moldenaers, P., Van Loey, A., & Hendrickx, M. (2009). Influence of intrinsic and extrinsic factors on rheology of pectin–calcium gels. *Food Hydrocolloids*, *23*(8), 2069–2077.

Fraeye, I., Duvetter, T., Doungla, E. N., Van Loey, A., & Hendrickx, M. (2010). Fine-tuning the properties of pectin–calcium gels by control of pectin fine structure, gel composition and environmental conditions. *Trends in Food Science & Technology*, *21*(5), 219–228.

Garnier, C., Axelos, M. A. V., & Thibault, J.-F. O. (1993). Phase diagrams of pectin–calcium systems: Influence of pH, ionic strength, and temperature on the gelation of pectins with different degrees of methylation. *Carbohydrate Research*, *240*(0), 219–232.

Glatter, O., & Kratky, O. (1982). *Small angle X-ray scattering*. London: Academic Press.

Grant, G. T., Morris, E. R., Rees, D. A., Smith, P. J. C., & Thom, D. (1973). Biological interactions between polysaccharides and divalent cations: The egg-box model. *FEBS Letters*, *32*(1), 195–198.

Hourdet, D., & Muller, G. (1991). Solution properties of pectin polysaccharides II. Conformation and molecular size of high galacturonic acid content isolated pectin chains. *Carbohydrate Polymers*, *16*(2), 113–135.

Iijima, M., Hatakeyama, T., & Hatakeyama, H. (2005). Swelling behaviour of calcium pectin hydrogels by thermomechanical analysis in water. *Thermochimica Acta*, *431*(1–2), 68–72.

Josef, E., & Bianco-Peled, H. (2012). Conformation of a natural polyelectrolyte in semidilute solutions with no added salt. *Soft Matter*, *8*(35), 9156–9165.

Kastner, H., Einhorn-Stoll, U., & Senge, B. (2012). Structure formation in sugar containing pectin gels – Influence of $Ca^{2+}$ on the gelation of low-methoxylated pectin at acidic pH. *Food Hydrocolloids*, *27*(1), 42–49.

Kim, W. J., Rao, V. N. M., & Smit, C. J. B. (1978). Effect of chemical composition on compressive mechanical properties of low ester pectin gels. *Journal of Food Science*, *43*(2), 572–575.

Krupa, I., Nedelcev, T., Racko, D., & Lacik, I. (2010). Mechanical properties of silica hydrogels prepared and aged at physiological conditions: Testing in the compression mode. *Journal of Sol–Gel Science and Technology*, *53*(1), 107–114 (LA – English)

Li, L., Fang, Y., Vreeker, R., Appelqvist, I., & Mendes, E. (2007). Reexamining the egg-box model in calcium-alginate gels with X-ray diffraction. *Biomacromolecules*, *8*(2), 464–468.

Liu, L., Fishman, M., & Hicks, K. (2007). Pectin in controlled drug delivery – A review. *Cellulose*, *14*(1), 15–24.

Luzio, G. A., & Cameron, R. G. (2008). Demethylation of a model homogalacturonan with the salt-independent pectin methylesterase from citrus. Part II. Structure–function analysis. *Carbohydrate Polymers*, *71*(2), 300–309.

Mitchell, J. R. (1980). The rheology of gels. *Journal of Texture Studies*, *11*(4), 315–337.

Morris, E. R., Powell, D. A., Gidley, M. J., & Rees, D. A. (1982). Conformations and interactions of pectins. I. Polymorphism between gel and solid states of calcium polygalacturonate. *Journal of Molecular Biology*, *155*(4), 507–516.

Munarin, F., Tanzi, M. C., & Petrini, P. (2012). Advances in biomedical applications of pectin gels. *International Journal of Biological Macromolecules*, *51*(4), 681–689.

Ngouamazong, D. E., Jolie, R. P., Cardinaels, R., Fraeye, I., Van Loey, A., Moldenaers, P., et al. (2012). Stiffness of $Ca^{2+}$–pectin gels: Combined effects of degree and pattern of methylesterification for various $Ca^{2+}$ concentrations. *Carbohydrate Research*, *348*, 69–76.

Ngouemazong, D. E., Nkemamin, N. F., Cardinaels, R., Jolie, R. P., Fraeye, I., Van Loey, A. M., et al. (2012). Rheological properties of $Ca^{2+}$-gels of partially methylesterified polygalacturonic acid: Effect of "mixed" patterns of methylesterification. *Carbohydrate Polymers*, *88*(1), 37–45.

Ngouemazong, D. E., Twngweh, F. F., Fraeye, I., Duvetter, T., Cardinaels, R., Van Loey, A. M., et al. (2012). Effect of de-methylestrification on network development and nature of $Ca^{2+}$ pectin gels: Toward understanding structure–function relations of pectin. *Food Hydrocolloids*, *26*(1), 89–98.

Pedersen, J. S., & Schurtenberger, P. (1996). Scattering functions of semiflexible polymers with and without excluded volume effects. *Macromolecules*, *29*(23), 7602–7612.

Powell, D. A., Morris, E. R., Gidley, M. J., & Rees, D. A. (1982). Conformations and interactions of pectins. II. Influence of residue sequence on chain association in calcium pectate gels. *Journal of Molecular Biology*, *155*(4), 517–531.

Rolin, C. (2002). commercial pectin preparations. In G. B. Seymour, & J. P. Knox (Eds.), *Pectins and their manipulation* (pp. 222–241). London: John Wiley & Sons, Limited.

Rubinstein, M., & Colby, R. H. (2003). *Polymer physics*. Oxford: Oxford University Press.

Schuster, E., Cucheval, A., Lundin, L., & Williams, M. A. K. (2011). Using SAXS to reveal the degree of bundling in the polysaccharide junction zones of microrheologically distinct pectin gels. *Biomacromolecules*, *12*(7), 2583–2590.

Siew, C. K., Williams, P. A., & Young, N. W. G. (2005). New insights into the mechanism of gelation of alginate and pectin: Charge annihilation and reversal mechanism. *Biomacromolecules*, *6*(2), 963–969.

Sriamornsak, P. (2003). Chemistry of pectin and its pharmaceutica uses: A review. *Silpakorn University International Journal*, *3*, 206–228.

Stokke, B. T., Draget, K. I., Smidsrod, O., Yuguchi, Y., Urakawa, H., & Kajiwara, K. (2000). Small-angle X-ray scattering and rheological characterization of alginate gels. 1. Ca-alginate gels. *Macromolecules*, *33*(5), 1853–1863.

Strom, A., Ribelles, P., Lundin, L., Norton, I., Morris, E. R., & Williams, M. A. K. (2007). Influence of pectin fine structure on the mechanical properties of calcium–pectin and acid–pectin gels. *Biomacromolecules*, *8*(9), 2668–2674.

Thibault, J. F., & Ralet, M. C. (2003). Physico-chemical properties of pectins in the cell walls and after extraction. In F. Voragen, H. Schols, & R. G. F. Visser (Eds.), *Advances in pectin and pectinase research* (pp. 91–105). Dordrecht, the Netherlands: Springer.

Thibault, J. F., & Rinaudo, M. (1986). Chain association of pectic molecules during calcium-induced gelation. *Biopolymers*, *25*(3), 455–468.

Tibbits, C. W., MacDougall, A. J., & Ring, S. G. (1998). Calcium binding and swelling behaviour of a high methoxyl pectin gel. *Carbohydrate Research*, *310*(1–2), 101–107.

Treloar, L. R. G. (1975). *The physics of rubber elasticity*. Oxford, GB: Clarendon Press.

Van Kleef, F. S. M., Boskamp, J. V., & Van Den Tempel, M. (1978). Determination of the number of cross-links in a protein gel from its mechanical and swelling properties. *Biopolymers*, *17*(1), 225–235.

Vincken, J.-P., Schols, H. A., Oomen, R. J. F. J., McCann, M. C., Ulvskov, P., Voragen, A. G. J., et al. (2003). If homogalacturonan were a side chain of rhamnogalacturonan. I. Implications for cell wall architecture. *Plant Physiology*, *132*(4), 1781–1789.

Zsivánovits, G., Marudova, M., & Ring, S. (2005). Influence of mechanical properties of pectin films on charge density and charge density distribution in pectin macromolecule. *Colloid and Polymer Science*, *284*(3), 301–308.